

Neuronal Excitability

# Function of Excitatory Periaqueductal Gray Synapses in the Ventral Tegmental Area following Inflammatory Injury

Claire Elena Manning, Michael Fritz, and Julie Ann Kauer

<https://doi.org/10.1523/ENEURO.0324-22.2022>

Nancy Pritzker Laboratory, Department of Psychiatry and Behavioral Sciences, Stanford University, Stanford, California 94305-5101

## Abstract

Manipulating the activity of ventral tegmental area (VTA) dopamine (DA) neurons can drive nocifensive reflexes, and their firing rates are reduced following noxious stimuli. However, the pain-relevant inputs to the VTA remain incompletely understood. In this study, we used male and female mice in combination with identified dopamine and GABA neurons in the VTA that receive excitatory inputs from the periaqueductal gray (PAG), a nexus of ascending pain information. We tested whether PAG–VTA synapses undergo functional plasticity in response to a pain model using optical stimulation in conjunction with slice electrophysiology. We found that acute carrageenan inflammation does not significantly affect the strength of excitatory PAG synapses onto VTA DA neurons. However, at the PAG synapses on VTA GABA neurons, the subunit composition of NMDA receptors is altered; the complement of NR2D subunits at synaptic sites appears to be lost. Thus, our data support a model in which injury initially alters synapses on VTA GABA neurons. Over time, these alterations may increase tonic inhibition of VTA DA neurons leading to their reduced firing.

**Key words:** carrageenan; glutamate; pain; periaqueductal gray; ventral tegmental area

## Significance Statement

Following a focal injury, the firing rate of dopamine neurons of the ventral tegmental area (VTA) decreases, despite a lack of direct innervation from the periphery. Here we assess the functional changes between a primary node of nociceptive output, the periaqueductal gray (PAG), and the VTA after peripheral inflammation. We find that synaptic strength at PAG-to-VTA dopamine neuron synapses is unaffected following inflammatory injury, but find a change in subunit composition of NMDARs at PAG synapses on the inhibitory neurons of the VTA.

## Introduction

Pain and analgesia are complex phenomena regulated at multiple sites in ascending and descending nociceptive pathways. Much has been uncovered at the level of the periphery and spinal cord itself, but the role of supraspinal structures in shaping pain perception and analgesia is not fully understood.

The ventral tegmental area (VTA) contains predominantly dopaminergic neurons and a prominent minority of

GABAergic neurons, as well as a small number of glutamatergic neurons (Nair-Roberts et al., 2008). During noxious pain events, most dopamine (DA) neurons are inhibited (Mirenowicz and Schultz, 1996; Ungless et al., 2004; Yang et al., 2021), while GABA neurons are excited (however, for discussion of noxious phasic excitation in DA neurons, see Brischoux et al., 2009). The intrinsic excitability of most DA neurons is unchanged in chronic pain models (Huang et al., 2019), despite reduced firing rates *in vivo* (Ren et al., 2016;

Received August 13, 2022; accepted November 28, 2022; First published December 7, 2022.

The authors declare no competing financial interests.

Author contributions: C.E.M. and J.A.K. designed research; C.E.M. and M.F. performed research; C.E.M. and M.F. analyzed data; C.E.M. and J.A.K. wrote the paper.

Watanabe et al., 2018) and a significant increase in inhibitory synaptic input to DA neurons (Markovic et al., 2021; Yang et al., 2021). Furthermore, silencing of VTA DA neurons reduces the strength or time needed for a stimulus to elicit nociceptive reflexes, while stimulation of these neurons during neuropathic pain models drives analgesic behavior (i.e., increased stimulation is required to elicit a nociceptive reflex and an increase is seen in time spent in a chamber associated with pain; Navratilova et al., 2012; Watanabe et al., 2018; de Jong et al., 2019; Taylor et al., 2019b; Waung et al., 2019; Sun et al., 2021). Within the VTA, opiate drugs act mainly through  $\mu$ -opioid receptors located on GABA neurons of the VTA where they act to disinhibit DA neurons (Johnson and North, 1992). Together, this information suggests a simple model in which inhibitory inputs onto dopamine neurons are the primary drivers of the neuroadaptations following pain experience. However, very few studies have considered functional changes in excitatory inputs onto either dopamine or GABA VTA neurons during a pain model. Furthermore, the source of nociceptive circuit inputs to VTA neurons are still being identified.

One input that is potentially relevant to nociception is the periaqueductal gray (PAG). A subset of spinal cord neurons carrying nociceptive information synapse directly within the PAG (Basbaum et al., 2009), making it a primary site for regulation of ascending nociceptive information. Furthermore, the PAG is a known nexus of ascending nociceptive information and opiate-mediated analgesia (Lewis and Gebhart, 1977; Mendes-Gomes et al., 2011; Champion et al., 2016). The PAG contains nonoverlapping populations of glutamatergic and GABAergic neurons, as well as a minority of monoaminergic neurons (Suckow et al., 2013; Samineni et al., 2017). All of these cell types have been implicated in pain modulation and the affective experience of pain, and these roles appear to depend on their projection targets and actions. For example, driving inhibitory PAG neurons facilitates nociception (Samineni et al., 2017), and inhibitory PAG projections to the amygdala contribute to fear learning and anxiety behaviors (Lowery-Gionta et al., 2018). Monoaminergic PAG neurons are critical in pain processing (Taylor et al., 2019a) in part through their projections to the amygdala (Li and Kash, 2019), whereas locally acting monoaminergic PAG neurons can drive freezing behavior (Vaaga et al., 2020). Driving excitatory PAG neurons suppresses nociception, as well as anxiety-related behavior (Samineni et al.,

2017; Taylor et al., 2019a). Together, these findings emphasize a pivotal role for the PAG and its afferents in pain experience.

Relatively little is known about the behavioral consequences of driving PAG projections to the ventral tegmental area. PAG afferents make both excitatory and inhibitory (but not monoaminergic projection) synapses on identified GABA and DA neurons of the VTA (Omelchenko and Sesack, 2010; Suckow et al., 2013; Ntamati et al., 2018; Waung et al., 2019). Furthermore, the inhibitory projections from the PAG to VTA DA neurons can undergo a unique opiate-sensitive long-term potentiation (LTP; St Laurent et al., 2020). This further indicates that PAG–VTA projections could be an important nexus of supraspinal functional changes during pain and pain relief. However, there is a dearth of evidence investigating this intriguing hypothesis. To date, and to our knowledge, only two behavioral studies have tested manipulation of the PAG–VTA circuit. The first reported that driving all PAG-to-VTA afferents is aversive, supporting conditioned place aversion. However, inhibition of these pathways is only reinforcing when animals are in a pain state (Waung et al., 2019). This finding further supports the hypothesis that this pathway undergoes functional plasticity in the context of pain. A second study found that specifically driving inhibitory PAG afferents to the VTA is not reinforcing in naive mice (St Laurent et al., 2020).

Together, these findings indicate a possible role for excitatory PAG–VTA inputs contributing to the negative affect associated with pain. At the synapse level, this could manifest either as a reduction in glutamatergic synaptic strength on VTA dopamine neurons, and/or an increase in glutamatergic synaptic strength on VTA GABA neurons. However, there are no studies on the functional changes in the excitatory PAG–VTA circuit following injury. Here we used an inflammatory pain model to assess changes in functional excitatory neurotransmission in the PAG-to-VTA circuit, specifically analyzing glutamatergic synapses onto both DA and GABA neurons. During inflammatory pain, we found no changes in excitatory synapse strength at PAG–VTA DA neurons, but report subtle changes at synapses on PAG–VTA GABA neurons. After inflammatory injury, the subunit composition of NMDA receptors (NMDARs) in these synapses on VTA GABAergic neurons is altered, with a reduced complement of NR2D subunits.

## Materials and Methods

### Animals

All experiments were performed with approval of protocols from Stanford University Institutional Animal Care and Use Committee. B6J.129S6(FVB)-Slc32a1<sup>tm2(Cre)Lowl</sup>/MwarJ (VGat-Cre; catalog #028862; <https://www.jax.org/strain/028862>), B6.Cg-Gt(ROSA)26Sor<sup>tm14(CAG-tdTomato)Hze</sup>/J (Ai14; catalog #007914; <https://www.jax.org/strain/007914>), and B6.129P2-Pitx3<sup>tm1Mli</sup>/Mmjax (Pitx3-GFP) (catalog #41479; <https://www.jax.org/strain/028554>) mice were obtained from The Jackson Laboratory and bred at Stanford University. Males and females were

This work was supported by the Stanford Neurochoice Initiative; National Institute on Drug Abuse Grants 5T32-DA-035165-08 (trainee; to C.E.M.) and DA-011289 (J.A.K.); and National Institute for Neurological Disorders and Stroke Grant 1F32-NS-123012-01 (to C.E.M.).

M. Fritz's present addresses: School of Health and Social Sciences, AKAD University of Applied Sciences, 70191 Stuttgart, Germany; and Department of Forensic Psychiatry and Psychotherapy, Ulm University, D-89069 Ulm, Germany.

Correspondence should be addressed to Julie Ann Kauer at [jkauer@stanford.edu](mailto:jkauer@stanford.edu).

<https://doi.org/10.1523/ENEURO.0324-22.2022>

Copyright © 2022 Manning et al.

This is an open-access article distributed under the terms of the Creative Commons Attribution 4.0 International license, which permits unrestricted use, distribution and reproduction in any medium provided that the original work is properly attributed.

**Table 1: Classification of sexes used in each analysis**

Experiment	Figure	Panels	Control		Experimental		Sum
			Female	Male	Female	Male	
Gq DREADD	1	C–E	3	3	3	3	12
Gi DREADD	1	F–H	3	4	4	2	13
Pain behavior 4 h	2	A–D	6	2	6	1	15
Pain behavior 24 h	2	E, F	2	5	2	6	15
DA neuron PPR	3	C, D	5	14	5	12	36
GABA neuron PPR	3	F, G	9	2	5	6	22
DA AMPA/NMDA	4	B	7	7	1	9	24
DA –70	4	C	9	13	3	15	40
DA +40	4	D	8	7	1	11	27
DA NASPM	4	E	4	8	4	6	22
GABA AMPA/NMDA	5	B	10	2	6	8	26
GABA –70	5	C	13	4	9	11	37
GB +40	5	D	11	3	7	8	29
GABA NASPM	5	E	8	0	2	3	13
GABA GLUN2D UBP	6	B, C	5	5	4	7	21
GABA GLUN2D ifenprodil	6	E, F	5	4	4	7	20

both used in experiments. Although we were not sufficiently powered to determine sex differences, we identify the number of samples from males and females in each experiment (Table 1). Mice were housed in a 12 h light/dark (LD) cycle and fed *ad libitum*.

### Intracranial injection surgery

Animals were deeply anesthetized with a mixture of ketamine (9 mg/kg) and xylazine (1 mg/kg). Two hundred nanoliters of the viral vector AAV-DJ-hSyn-ChR2-eYFP ( $5.78 \times 10^{12}$ ) was bilaterally targeted to the ventrolateral PAG (vIPAG) of postnatal day 21 (P21) to P28 animals [anteroposterior (AP),  $-3.73$ ; mediolateral (ML),  $\pm 0.4$ ; dorsoventral (DV),  $-2.29$ ;  $0^\circ$  angle] for all electrophysiology studies. For behavioral assays, 200 nl of AAV5.pENN.AAV.CamKII 0.4.Cre.SV40 [ $7 \times 10^{12}$  viral genomes (vg/ml)] were targeted to the adult vIPAG, as follows: (AP,  $-4.9$ ; ML,  $\pm 0.5$ ; DV,  $-2.7$ ), and 400 nl of pAAVrg-hSyn-DIO-hM4D(Gi)-mCherry ( $8 \times 10^{12}$  vg/ml), pAAVrg-hSyn-DIO-hM3D(Gq)-mCherry ( $7 \times 10^{12}$  vg/ml), or pAAVrg-hSyn-DIO-EGFP ( $7 \times 10^{12}$  vg/ml) retrogradely expressing virus into the VTA (AP,  $-3.0$ ; ML,  $\pm 0.45$ ; DV,  $-4.6$ ). Following surgery, the animals recovered for at least 3 weeks to obtain adequate viral expression.

### Hindpaw injections

Mice were anesthetized with 5% isoflurane until a lack of toe-pinch reflex was observed. Then, under 3% isoflurane, the hindpaws of the animals were disinfected with 70% ethanol and a betadine scrub. Following cleaning, either 1% carrageenan in 0.9% saline or saline alone was administered into both hindpaws at  $5 \mu\text{l/g}$  body weight using a 30 ga needle.

### Behavioral testing

Behavioral testing was performed between the hours of 10:00 A.M. to 5:00 P.M. during the lights-on period under either dim or white light conditions in adult animals.

### von Frey

von Frey testing was performed according to the SUDO (simplified up-down) method (Bonin et al., 2014). Briefly, animals were placed on a mesh screen, and filaments were presented to elicit a withdrawal reflex. An absence of reflex was followed by a smaller filament presentation and vice versa. Animals were exposed to a total of five stimulus presentations per paw.

### Static hot plate

Animals were placed on a hot plate heated to  $55^\circ\text{C}$ , and the latency to hindpaw licking, biting, grooming, or attempted escape from the plate (nocifensive behaviors) was recorded. The trials were terminated at 20 s.

### Dynamic hot plate

Animals were placed on plate at a warm, but not noxious, temperature ( $30^\circ\text{C}$ ). This temperature was then ramped at a rate of  $2.5^\circ/\text{min}$  to  $55^\circ\text{C}$ . The trial ended when the animal displayed a nocifensive behavior or when the plate reached  $55^\circ\text{C}$ , whichever occurred first.

### Elevated plus maze

Animals were placed in the center of the elevated plus maze (EPM) and were allowed to roam under low-light conditions for 10 min. The amount of time spent in the open arms were recorded and scored on Biobserve Software. Animals were injected with 1 mg/kg clozapine-*N*-oxide (CNO; Enzo Life Sciences) 15 min before the start of behavioral testing.

### Light/dark box

Animals were placed in the dark portion of the Light/Dark (LD) box ( $20 \times 40$  cm) and allowed to roam for 10 min. The latency to enter the light side of the chamber was recorded. Animals were injected with 1 mg/kg CNO 15 min before the start of the behavioral experiments.

### Conditioned place preference

Animals were run in dim light conditions. Pretest, animals were placed in the center chamber of a three-chamber apparatus and allowed to explore freely for 15 min.

For the next 5 d, animals were conditioned in the morning to 0.9% saline (i.p.) while confined to one side of the chamber and 1 mg/kg CNO (i.p.) while confined to the other side in the afternoons at 30 min per conditioning session. During the post-test, animals freely roamed, drug free, for another 15 min, and time spent on each side of the chamber was measured.

### Brain slice preparation

Horizontal midbrain slices (220  $\mu\text{m}$ ) were prepared from 6- to 9-week-old male and female mice 3–6 weeks following viral injection. Animals were deeply anesthetized with drop isoflurane and overdosed with ketamine (37.5 mg/kg) before cardiac perfusion with the following ice-cold oxygenated choline slicing solution (in mM): 110 choline chloride, 25 glucose, 25  $\text{NaHCO}_3$ , 7  $\text{MgCl}_2$ , 11.6 sodium ascorbate, 3.1 sodium pyruvate, 2.5 KCl, 1.25  $\text{NaH}_2\text{PO}_4$ , and 0.5  $\text{CaCl}_2$  saturated with 95%  $\text{O}_2$ /5%  $\text{CO}_2$ , at pH 7.4 and 290–300 mOsm. Brains were rapidly removed and sliced (0.12 mm/s) on a vibratome (model 1200S, Leica). Slices recovered for 10 min at 37°C in the following oxygenated aCSF (in mM): 126 NaCl, 21.4  $\text{NaHCO}_3$ , 2.5 KCl, 1.2  $\text{NaH}_2\text{PO}_4$ , 2.4  $\text{CaCl}_2$ , 1.0 Mg  $\text{SO}_4$ , 11.1 glucose, and 5 sodium ascorbate. Slices were then held in the same solution at room temperature for up to 8 h until being transferred to a recording chamber.

### Electrophysiology

Brain slices were continuously perfused with oxygenated aCSF (28–32°C) containing 1  $\mu\text{M}$  strychnine and 20  $\mu\text{M}$  bicuculline to block glycine and  $\text{GABA}_A$  receptors, respectively. Dopaminergic neurons were identified via fluorescent labeling in Pitx3-GFP mice (van den Munckhof et al., 2003; Zhao et al., 2004), while  $\text{GABA}_B$  neurons were identified in slices from *vgat-Cre*  $\times$  *Ai14* mice (Madisen et al., 2010; Stuber et al., 2015; Root et al., 2018). Whole-cell recordings were performed with patch pipettes (1.8–4 M $\Omega$ ) containing Kgluc internal solution as follows (in mM): 117 K-gluconate, 2.8 NaCl, 5  $\text{MgCl}_2$ , 2 ATP-Mg, 0.3 GTP-Na, 0.6 EGTA, and 10 HEPES or CsCl internal solution (in mM): 125 CsCl, 2.8 NaCl, 2  $\text{MgCl}_2$ , 2 ATP-Na, 0.3GTP-Na, 0.6 EGTA, and 10 HEPES and voltage clamped at  $-70$  mV. AMPA/NMDA experiment recordings were performed with the CsCl internal solution, and cells were voltage clamped at  $-70$  and  $+40$  mV. In some experiments, QX314 (5 mM) was added to the internal solution. Although  $\text{GABA}_B$  receptors were not blocked, we did not observe synaptic currents at  $-70$  mV, which is consistent with slow  $\text{GABA}_B$  kinetics (Nugent et al., 2009). Additionally, currents were confirmed to be glutamatergic using AP-5 and NBQX where possible, and, as can be seen in Figures 4A and 5A, there was no residual current in these drugs at  $+40$  mV. Thus, all reported synaptic currents were presumed glutamatergic EPSCs.

### Stimulation protocols

Channelrhodopsin (ChR)-induced optically evoked EPSCs (oEPSCs) were evoked through the microscope objective using full-field light pulses from a white LED (Mightex) controlled by a driver (ThorLabs) and reflected through a 40 $\times$

water-immersion lens (Polter et al., 2018). All light pulses were of 10 ms duration across experiments to normalize exposure to blue light. Stimulation with pairs of oEPSCs (separated by 50 ms) were separated by 30 s to avoid desensitization of the opsin. The series resistance was monitored continuously during the experiment, and cells were discarded for deviations  $>15\%$ .

### AMPA/NMDA ratios

Cells were held at  $-70$  mV, and EPSCs were optically evoked to obtain a stable 10 min baseline. The GluA2-lacking AMPAR-specific antagonist NASPM (20  $\mu\text{M}$ ) was then bath applied for 10 min, followed by a 10 min application of the AMPAR antagonist NBQX (10  $\mu\text{M}$ ). Cells were then clamped at  $+40$  mV to record the total NMDAR current, followed by a 10 min application of the NMDAR2C/2D antagonist UBP141 (3  $\mu\text{M}$ ) and then the NMDAR2B antagonist ifenprodil (10  $\mu\text{M}$ , 10 min). Finally,  $\text{D-AP-5}$  (50  $\mu\text{M}$ ) was bath applied to confirm that all remaining currents were blocked. Optically evoked EPSCs often had multiple EPSC peaks, and AMPA/NMDA ratios were calculated using the initial peak amplitude from an average of five trials. The responses to NASPM and UBP141 were calculated from an average of five trials at 10 min following bath application of each drug. Drug effects were quantified as the percentage peak EPSC remaining in each drug compared with the EPSC before that drug was applied (10 min prior).

### Statistics

Results are shown as the mean  $\pm$  SEM. Significance was determined using one-variable parametric (Student's *t* tests) or nonparametric comparisons (Mann–Whitney *U* test), depending on data variance. When repeated-measures (RM) two-way ANOVAs were appropriate, they were followed by *post hoc* multiple comparisons where  $p < 0.05$ . Paired-pulse ratios (PPRs) were calculated using the mean EPSC2 amplitude divided by the mean EPSC1 amplitude for all trials. Coefficient of variation ( $1/\text{CV}^2$ ) was determined by dividing the EPSC1 mean amplitude squared by the mean variance. AMPA/NMDA ratios were calculated by comparing the basal peak amplitude at  $-70$  mV with its value 10 min following the application of NBQX and dividing this value by the difference between the basal value at  $+40$  mV before  $\text{D-AP-5}$ . Data were analyzed using GraphPad Prism (9.3.1)

## Results

The glutamatergic subpopulation of the vIPAG/dorsal raphe (DR) area has been previously implicated in controlling the behavioral responses to aversive stimuli. Here we first tested the role of driving or inhibiting glutamatergic vIPAG/DR afferents to the VTA in valenced behavior. We used a dual-viral strategy to selectively express either designer receptors exclusively activated by designer drugs (DREADDs) or a reporter in glutamatergic cells of the PAG/DR that project to the VTA (Fig. 1A,B), and CNO injections (1 mg/kg) were then delivered to exert control over the circuit. pAAV5.pENN.AAV.CamKII 0.4.Cre.SV40 was targeted to the PAG, while pAAVrg-hSyn-DIO-hM4D (Gi)-mCherry, pAAVrg-hSyn-DIO-hM3D(Gq)-mCherry, or

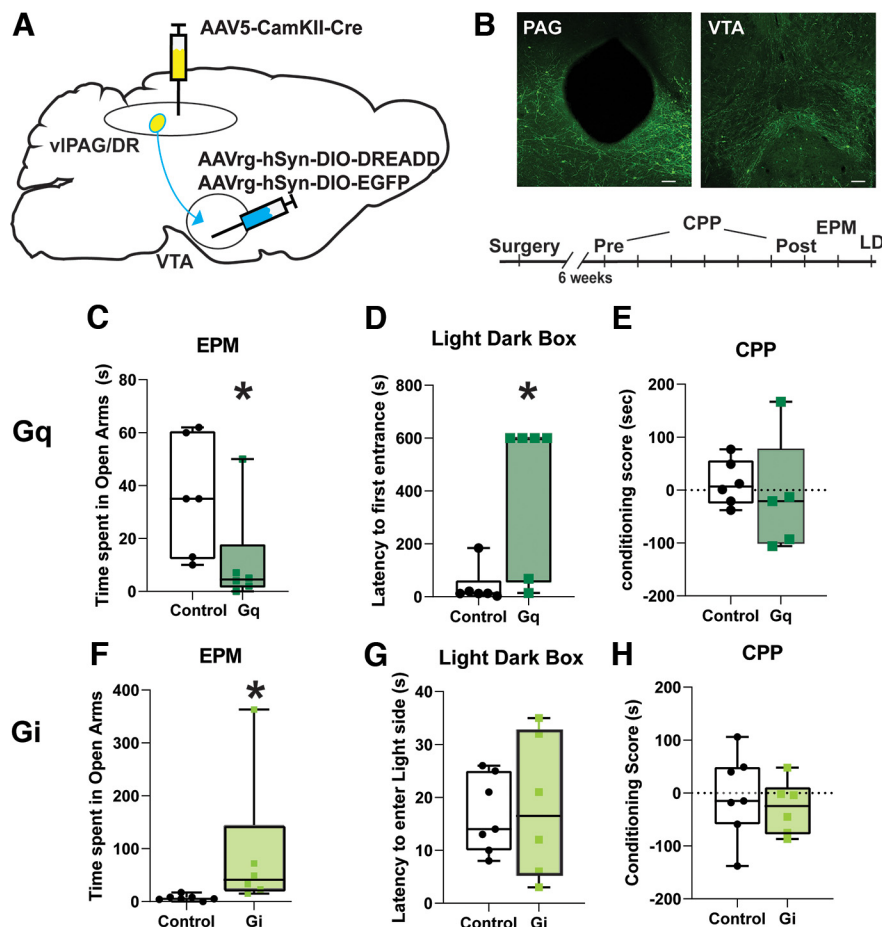


**Figure 1.** Driving excitatory vIPAG/DR afferents to the VTA reduces exploratory behavior. **A**, A schematic for the exclusive expression of DREADDs in excitatory PAG/DR projections to the VTA. **B**, An example of targeting in the PAG (above left) and the expression of terminals in VTA (above right) and the timeline of behavioral assessments (below). In some cohorts, the order of the LD and EPM assays were alternated. **C**, After CNO administration, mice expressing Gq DREADDs spent less time in the open arms of the elevated plus maze compared with control animals (Mann–Whitney test:  $U=5$ ,  $p=0.0216$ ). **D**, These Gq DREADD-expressing mice also had increased latencies to enter the light side of a light/dark box ( $U=4$ ,  $p=0.013$ ). **E**, CNO administration did not alter CPP scores in these mice (Mann–Whitney test:  $U=9.5$ ,  $p=0.355$ ). **F**, When mice expressing Gi DREADDs in this pathway were exposed to CNO, they significantly increased the time spent in the open arms of the elevated plus maze compared with mice expressing a control virus (Mann–Whitney test:  $U=2$ ,  $p=0.0017$ ). **G**, **H**, The same mice showed no differences in the time to enter the light side of the LD chamber (Mann–Whitney test:  $U=20.5$ ,  $p=0.9755$ ; **G**) or in the CPP (Mann–Whitney test:  $U=17$ ,  $p=0.6282$ ; **H**). \* $p < 0.05$ . Scale bar, 100  $\mu\text{m}$ .

pAAVrg-hSyn-DIO-EGFP were directed to the VTA. Driving the vIPAG/DR–VTA circuit with the excitatory Gq-coupled DREADD decreased the amount of time spent in the open arms of EPM (Fig. 1C; Mann–Whitney test:  $U=5$ ,  $p=0.0216$ ) and increased the latency to enter the light side of an LD box (Fig. 1D; Mann–Whitney test:  $U=4$ ,  $p=0.013$ ). We also tested for a rewarding/aversive response to driving this pathway using a conditioned place preference (CPP) assay. After a pretest during which mice were allowed to freely explore, mice were conditioned to one side of a three-chamber apparatus with saline and the other side with CNO for 5 d. On the following day, no drug was delivered, and the time spent in each chamber was measured. Place preference scores did not differ between saline and CNO paired chambers (Fig. 1E; Mann–Whitney test:  $U=9.5$ ,  $p=0.355$ ).

Conversely, DREADD-mediated inhibition of this pathway significantly increased the time spent in the open arms of the EPM (Fig. 1F; Mann–Whitney test:  $U=2$ ,  $p=0.0017$ ) but did not change the latency to enter the light side of chamber (Fig. 1G; Mann–Whitney test:  $U=20.5$ ,  $p=0.9755$ ). Similar to the results with the Gq-coupled DREADD, inhibiting this pathway over 2 d also did not affect CPP (Fig. 1H; Mann–Whitney test:  $U=17$ ,  $p=0.6282$ ). Our data affirm that vIPAG/DR glutamate neurons have a role in an anxiety-like response in mice (Taylor et al., 2019a) and demonstrate that this is mediated through its output to the VTA. Furthermore, our results are consistent with the idea that the vIPAG/DR-to-VTA excitatory afferents might be functionally altered during peripheral injury as pain from inflammatory injury often produces a negative affective state (Hummel et al., 2008; Burek et al., 2022), and we next tested this idea.

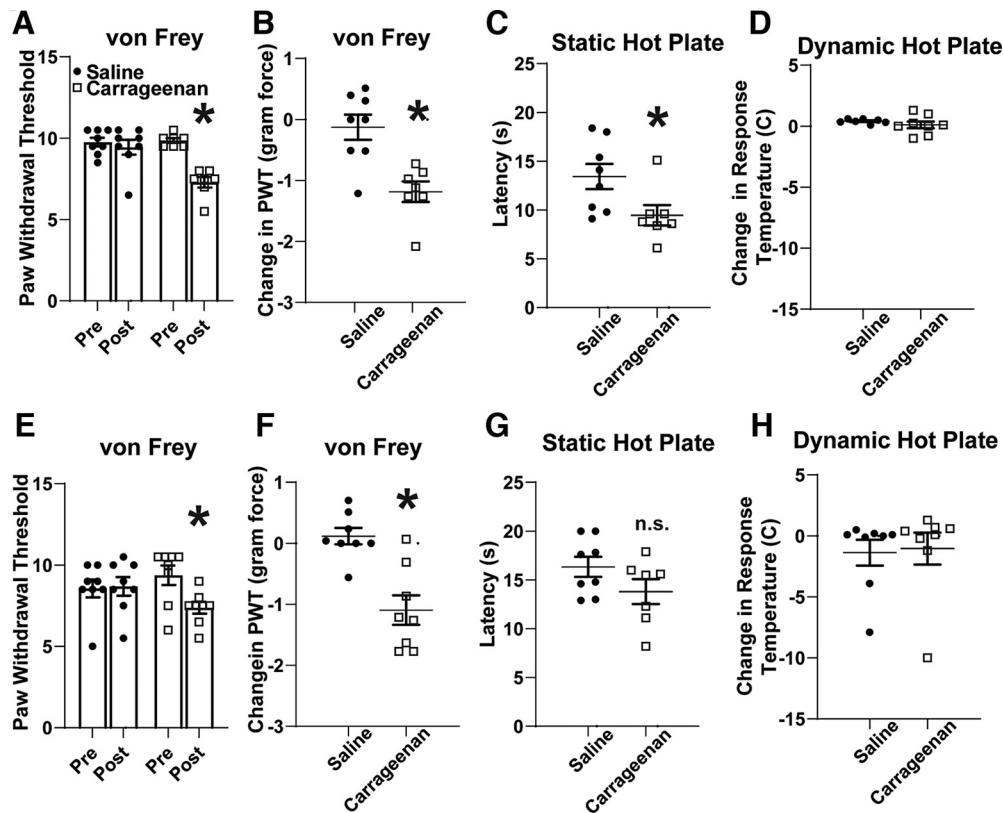


**Figure 2.** Carrageenan injection into the hindpaws produced mechanical hypersensitivity at 4 and 24 h postinjection. **A**, There was a significant interaction between hindpaw injection and time as assessed by two-way RM ANOVA (interaction:  $F_{(1,13)} = 17.46$ ,  $p = 0.001$ ). **B**, Sidak *post hoc* tests revealed that carrageenan-treated mice displayed a paw withdrawal reflex to significantly smaller von Frey filaments compared with saline-treated mice (carrageenan,  $p < 0.001$ ; saline,  $p = 0.655$ ;  $N = 15$ ) with significantly less force required to elicit the paw withdrawal threshold (Student's *t* test unpaired *t* test,  $p = 0.002$ ). **C**, **D**, At 4 h postinjection, carrageenan-treated mice also displayed a significantly reduced latency to nocifensive behaviors on a static hot plate (Student's *t* test unpaired *t* test,  $p = 0.035$ ; **C**), but no change in the temperature was required to elicit these behaviors ( $p = 0.342$ ; **D**). **E**, **F**, At 24 h, mice treated with carrageenan had a reduced paw withdrawal [RM two-way ANOVA,  $F_{(1,14)} = 10$ ,  $p = 0.0062$ , followed by Sidak *post hoc* tests (carrageenan  $p = 0.0256$ ); **E**] and corresponding to reduced force required to elicit paw withdrawal (Student's *t* test,  $p = 0.0006$ ; **F**). **G**, **H**, The thermal hypersensitivity was no longer significantly different for static hot plate (Student's *t* test unpaired *t* test,  $p = 0.14$ ) or for dynamic hot plate (Student's *t* test unpaired *t* test,  $p = 0.844$ ). \* $p < 0.05$ ; n.s.  $> 0.05$ .

### Mice injected with 1% carrageenan have mechanical hypersensitivity 24 h after exposure

To address functional changes in excitatory PAG-VTA projections following peripheral injury, we leveraged the inflammatory agent  $\lambda$ -carrageenan. When carrageenan is injected into the hindpaw, its maximal nociceptive effect is present at 4 h with resolution at 1–2 d (Benitz and Hall, 1959; Hargreaves et al., 1988; Deuis and Vetter, 2016), and the resultant edema is resolved within a week. We first validated this model in our own hands and assessed thermal and mechanical sensitivity 4 h after injection. In the von Frey assay, carrageenan-treated mice, but not saline-treated mice, had a significantly reduced paw withdrawal threshold (Fig. 2A; two-way RM ANOVA: interaction  $F_{(1,13)} = 17.46$ ,  $p = 0.001$ ; and Sidak *post hoc* test: carrageenan,  $p < 0.001$ ; saline,  $p = 0.655$ ;  $N = 15$ ). This directly corresponded to the reduction in mechanical force required for this reflex in carrageenan-treated mice (Fig. 2B; unpaired *t* test:  $p = 0.002$ ,  $N = 15$ ). In addition, these animals had thermal sensitivity, with carrageenan-

treated animals displaying a reduced latency to nocifensive behaviors on a static hot plate (Fig. 2C; unpaired *t* test;  $p = 0.035$ ,  $N = 15$ ). We also used a dynamic hot plate assay but did not observe a change in the temperature required to elicit nocifensive behaviors (Fig. 2D; unpaired *t* test;  $p = 0.342$ ,  $N = 15$ ). Together, our C57BL6 mice display mechanical and thermal sensitivity phenotypes 4 h after the injection of a 1% carrageenan solution into the hindpaws.

We also tested the effects of carrageenan on behavior at a 24 h time point. The mechanical hypersensitivity phenotype persisted at 24 h (Fig. 2E; two-way RM ANOVA: interaction,  $F_{(1,14)} = 10$ ,  $p = 0.006$ ; and Sidak *post hoc* test: carrageenan,  $p = 0.026$ ; saline,  $p = 0.983$ ;  $N = 16$ ; Fig. 2F; unpaired *t* test,  $p < 0.001$ ,  $N = 16$ ), although the thermal sensitivity phenotype resolved at this time point (Fig. 2G, H; unpaired *t* test;  $p = 0.14a$ ,  $p = 0.844b$ ;  $N = 16$ ), which is consistent with previous reports (Benitz and Hall, 1959; Deuis and Vetter, 2016). Therefore, the mice remain in a state of mechanical hypersensitivity at 24 h.

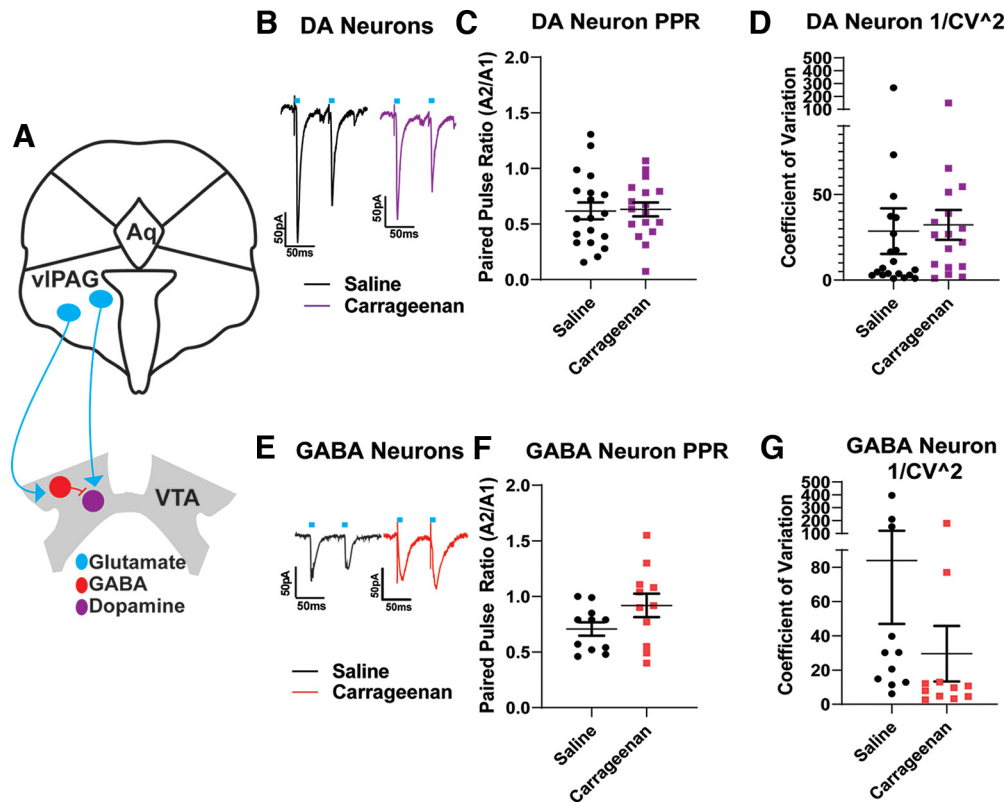


**Figure 3.** Excitatory periaqueductal gray afferents to the VTA do not display changes in presynaptic function following carrageenan injury. **A**, A schematic of PAG innervation of the VTA. **B**, Representative traces of oEPSCs onto VTA DA neurons from saline-treated (black) and carrageenan-treated (magenta) animals. Ten microsecond light pulses are denoted by the blue bar in this and all figures. **C, D**, When measuring PAG–VTA oEPSCs onto DA neurons, neither PPRs (Student’s *t* test unpaired *t* test,  $p = 0.89$ ) nor the coefficient of variation ( $1/CV^2$ ; Student’s *t* test unpaired *t* test,  $p = 0.8266$ ) is changed 24 h following carrageenan injection compared with saline controls. **E**, Representative traces of oEPSCs from VTA GABA neurons from saline-treated and carrageenan-treated animals. **F, G**, Cells from carrageenan-treated animals did not exhibit significant changes in paired-pulse ratio (Student’s *t* test unpaired *t* test,  $p = 0.098$ ) or  $1/CV^2$  (Student’s *t* test unpaired *t* test,  $p = 0.193$ ) compared with saline controls.

### Periaqueductal gray afferents to the VTA do not display changes in presynaptic function following carrageenan inflammation

We hypothesized that after inflammatory injury, excitatory synapses on VTA DA neurons may be weakened, and/or excitatory synapses on VTA GABAergic neurons might be strengthened. We first investigated presynaptic function at synapses onto either DA or GABA neurons within the VTA after carrageenan inflammation. To selectively label excitatory PAG afferents, we virally expressed cre-dependent Chr2. In VTA slices, we delivered optical stimulation while recording from fluorescently labeled VTA DA or GABA neurons. When measuring PAG–VTA oEPSCs on DA neurons, neither paired-pulse ratios (PPRs) nor the coefficient of variation were changed at 24 h following inflammatory injury (Fig. 3C,D; unpaired *t* test:  $p = 0.89$ ;  $p = 0.8266$ ;  $n = 36$  cells,  $N = 16$  animals). Similarly, PAG–VTA oEPSCs on GABA neurons did not show significant changes 24 h following injury, despite a trend toward increased PPR and decreased  $1/CV^2$  (Fig. 3F,G; unpaired *t* test:  $p = 0.098$ ;  $p = 0.193$ ;  $n = 22$  cells,  $N = 16$  animals). Together, these results suggest that, following acute inflammation, glutamate release probability at synapses on VTA dopamine or GABA neurons is not likely affected.

### Acute inflammation does not alter postsynaptic responses at PAG synapses onto VTA DA neurons

We next tested whether injury-induced reductions in glutamatergic PAG–VTA synaptic strength on DA neurons may arise instead through changes in postsynaptic glutamate receptors. First, we measured AMPA/NMDA ratios at these synapses, but found no differences between the cells from saline-treated or carrageenan-treated animals (Fig. 4B; unpaired *t* test,  $p = 0.503$ ; cells,  $N = 25$ ; animals,  $N = 17$ ). Of note, a subset of these cells had very small NMDA currents despite large AMPA currents, contributing to large AMPA/NMDA ratios. We then investigated the contributions of individual types of glutamate receptors. We found no differences between groups in the amount of current passed at  $-70$  mV (presumed AMPA-mediated currents) or at  $+40$  mV coupled with bath application of NBQX (Fig. 4C,D; presumed NMDAR currents; unpaired *t* test:  $p = 0.76$ ; cells,  $N = 40$ ; animals,  $N = 27$ ;  $p = 0.1213$ ; cells,  $N = 27$ ; animals,  $N = 25$ ). VTA DA neurons are also known to express calcium-permeable (CP) AMPA receptors (AMPA<sub>CP</sub>; also known as GluA2-lacking AMPARs; Bellone and Lüscher, 2006), which are implicated in forms of synaptic plasticity (Liu and Zukin, 2007). Therefore, we also examined whether there were functional changes in

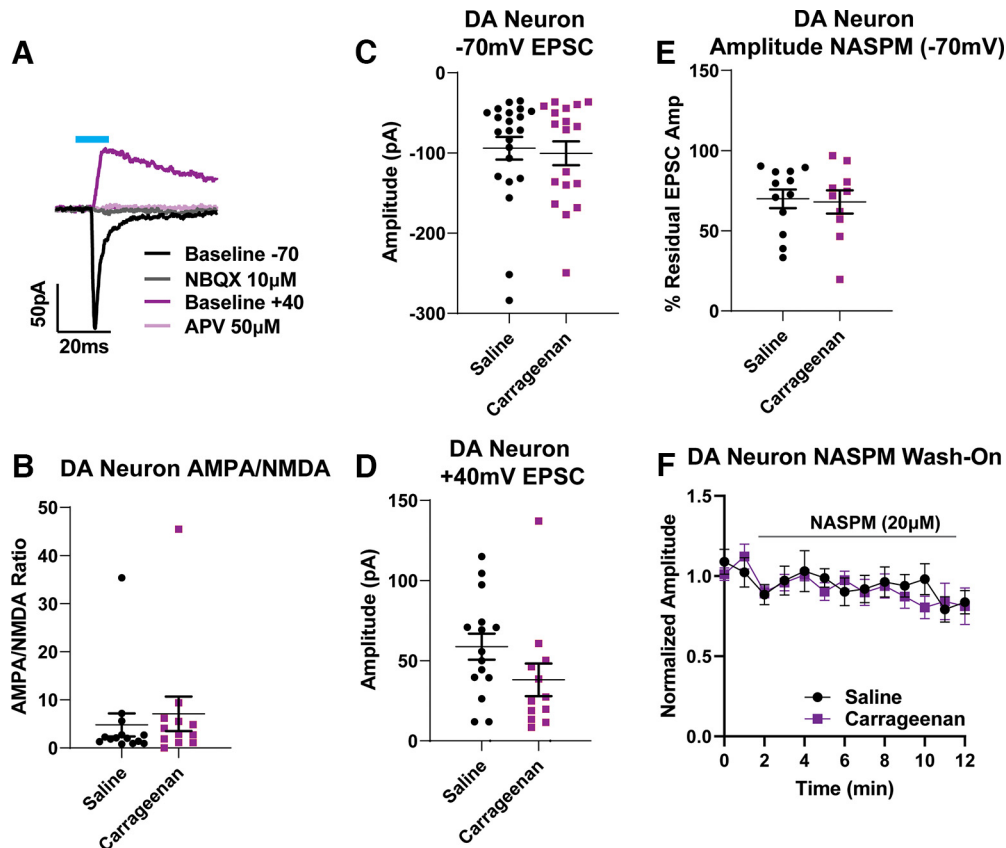


**Figure 4.** PAG–VTA oEPSCs on DA neurons are unchanged following carrageenan injury. **A**, Representative example of the optically evoked current protocol used to measure AMPA/NMDA ratios in DA cells. After recording currents at  $-70$  mV (black), NBQX was added (gray); after depolarizing the cell to  $+40$  mV (magenta), D-AP-5 was applied (pink; see Materials and Methods). **B**, AMPA/NMDA ratios at these synapses were not different between saline-treated and carrageenan-treated groups (Student’s *t* test unpaired *t* test,  $p = 0.503$ ). **C**, Average evoked AMPA currents did not differ between the two groups (Student’s *t* test unpaired *t* test,  $p = 0.76$ ). **D**, Average evoked NMDAR currents from carrageenan-treated animals were not significantly different compared with saline controls (Student’s *t* test unpaired *t* test,  $p = 0.1213$ ). **E**, Application of NASPM did not differentially affect oEPSCs at PAG–VTA synapses (Student’s *t* test unpaired *t* test,  $p = 0.83$ ). **F**, Time course of NASPM on oEPSCs at PAG–VTA synapses.

AMPA/NMDA ratios at PAG–VTA<sub>DA</sub> synapses using the CP-AMPA-specific antagonist NASPM. In the majority of DA cells, EPSCs were reduced by NASPM. However, we observed no differences between cells from saline or carrageenan animals (Fig. 4E,F; unpaired *t* test,  $p = 0.83$ ; cells,  $N = 22$ ; animals,  $N = 16$ ). Together, these data do not support the hypothesis that acute inflammatory injury alters overall excitatory drive from PAG neurons onto VTA dopamine neurons following an acute inflammatory injury.

**Acute inflammation does not alter postsynaptic responses at PAG synapses onto VTA GABA neurons**

Many VTA GABA neurons act as local interneurons, effectively controlling the output of DA cells. We therefore next tested whether inflammation results in increased strength of excitatory PAG synapses onto GABAergic VTA neurons. Using the same optogenetic approach to drive excitatory PAG afferents, we examined postsynaptic receptor contributions in identified VTA GABA cells. Again, there were no significant differences between saline-treated and carrageenan-treated cells in AMPA/NMDA ratios, EPSC amplitudes at  $-70$  mV, EPSC amplitudes at

$+40$  mV in the presence of NBQX, or responses to the CP-AMPA antagonist NASPM (Fig. 5B–F; unpaired *t* test:  $p = 0.806b$ ; cells,  $N = 28$ ; animals,  $N = 15$ ;  $p = 0.736c$ ; cells,  $N = 37$ ; animals,  $N = 23$ ;  $p = 0.561d$ ; cells,  $N = 30$ ; animals,  $N = 15$ ;  $p = 0.31e$ ; cells,  $N = 13$ ; animals,  $N = 7$ ). Together, our data do not support changes in postsynaptic drive at excitatory PAG synapses onto VTA GABA neurons following an acute inflammatory injury.

**Acute inflammation decreases the functional contribution of GluN2D containing NMDARs to PAG–VTA synapses on GABA neurons**

In the previous experiments, we considered NMDARs as classic GluN1/2A or GluN1/GluN2B heteromers. However, midbrain neurons also express the GluN2D subunit into adulthood, evidenced by electrophysiology and *in situ* hybridization (Monyer et al., 1994; Morris et al., 2018). In neurons containing the GluN2D subunits, the Mg<sup>2+</sup> block is weaker, allowing ionic flux at more negative membrane potentials but passing less Ca<sup>2+</sup> compared with GluN2B-containing receptors (Hansen et al., 2018). During our experiments recording from VTA GABAergic neurons,

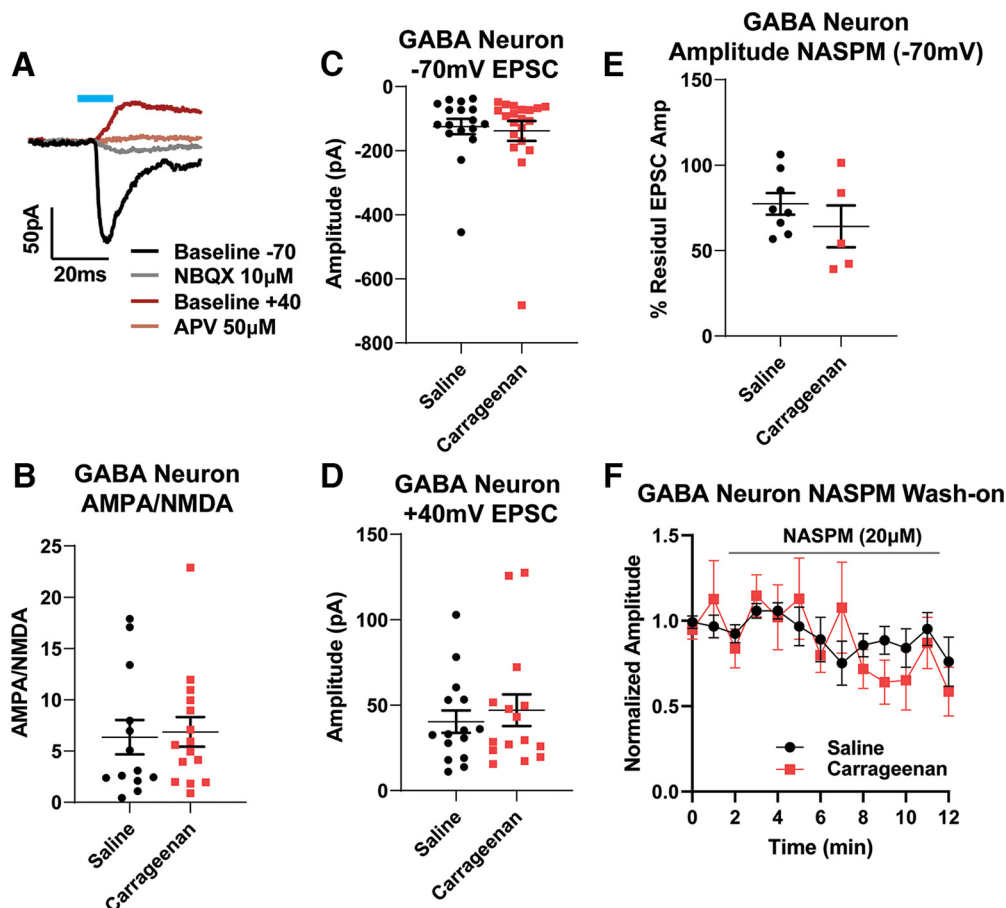


**Figure 5.** Carrageenan injury does not alter PAG–VTA oEPSCs on GABA neurons. **A**, Representative example of the optically evoked current protocol used to measure AMPA/NMDA ratios in GABA cells. After recording currents at  $-70$  mV (black), NBQX was added (gray); after depolarizing the cell to  $+40$  mV (dark red), APV was applied (brown; see Materials and Methods). **B**, AMPA/NMDA ratios at these synapses were not different between saline-treated and carrageenan-treated groups (Student’s *t* test unpaired *t* test,  $p = 0.806$ ). **C**, Average evoked AMPA currents were not different between these two groups (Student’s *t* test unpaired *t* test,  $p = 0.736$ ). **D**, Average evoked NMDAR currents from carrageenan-treated animals did not differ from saline controls (Student’s *t* test unpaired *t* test,  $p = 0.561$ ). **E**, Application of NASPM did not differentially affect oEPSCs at PAG–VTA synapses and GABA synapses (Student’s *t* test unpaired *t* test,  $p = 0.31$ ). **F**, Time course of NASPM on oEPSCs at PAG–VTA synapses.

we observed measurable inward NMDAR currents at  $-70$  mV, suggesting a contribution of GluN2D subunits at synapses from PAG afferents. Therefore, we next assessed whether the NMDARs at PAG–VTA GABA synapses were differentially sensitive to the GluN2D antagonist UBP141 or GluN2B antagonist ifenprodil. NMDAR currents in GABAergic neurons from carrageenan-treated mice lost their sensitivity to the GluN2D antagonist UBP141 ( $3 \mu\text{M}$ ) compared with cells from control animals as measured by either peak amplitude (Fig. 6B;  $p = 0.0091$ ; cells,  $N = 21$ ; animals,  $N = 15$ ), or total charge (Fig. 6C;  $p = 0.0055$ ; cells,  $N = 21$ ; animals,  $N = 15$ ). In contrast, these NMDAR currents were not significantly different in sensitivity to the GluN2B-specific antagonist ifenprodil ( $10 \mu\text{M}$ ) measured by peak amplitude (Fig. 6E;  $p = 0.1210$ ; cells,  $N = 20$ ; animals,  $N = 15$ ) and total charge in response to optogenetic stimulation (Fig. 6F;  $p = 0.0556$ ; cells,  $N = 20$ ; animals,  $N = 15$ ), although we noted a trend toward a greater ifenprodil response (EPSC amplitude,  $p = 0.12$ ; EPSC charge,  $p = 0.06$ ). Together, our data suggest that at this time point following

acute inflammation, the proportion of NMDARs containing the GluN2B subunit is not significantly changed, but there are fewer NMDARs containing the GluN2D subunit.

## Discussion

### PAG–VTA roles

Through bidirectional modulation of PAG glutamatergic inputs to VTA, we have shown a causal relationship between glutamatergic PAG–VTA and anxiety-like phenotypes both in the EPM and the LD box. Previously, the glutamatergic neurons of the PAG have been highlighted as contributing to anxiety-like phenotypes, but the relevant afferents had not been discovered (Taylor et al., 2019a). We did not, however, observe that chemogenetically activating PAG–VTA excitatory afferents affects place preference (Wang et al., 2019), indicating that stimulation of this pathway is valence neutral. Therefore, driving this afferent population may cause an attenuation of exploratory behavior, which can serve a protective role following

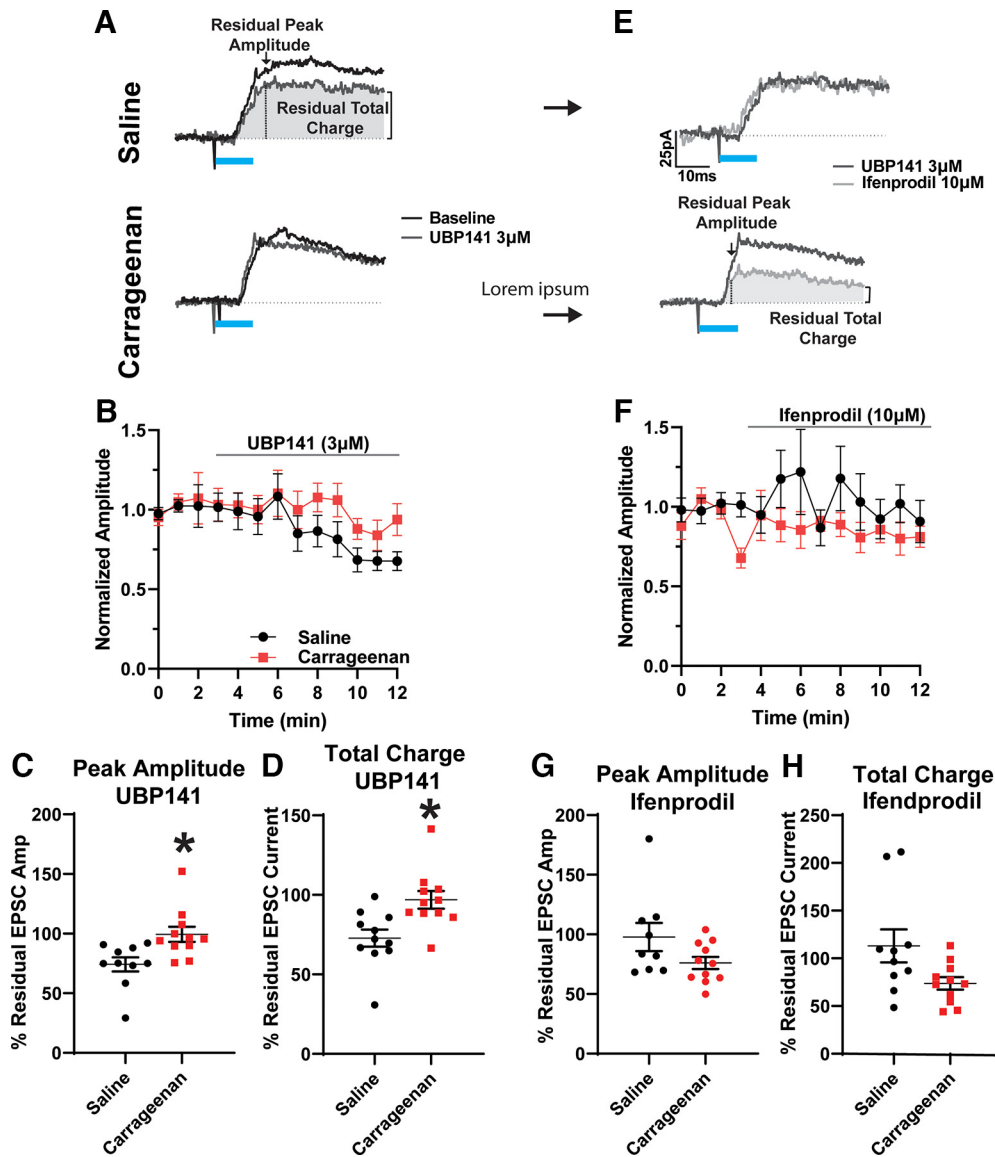


**Figure 6.** NMDA receptor subunits at PAG synapses on VTA GABA neurons are altered after injury. **A**, Representative example oEPSCs before and after bath application of UBP141 in GABA neurons from saline-treated (left) or carrageenan-treated (right) animals. **B**, Time course of isolated peak amplitudes of NMDAR oEPSCs following bath application of UBP141 (3  $\mu$ M), a GluN2D antagonist, quantified in **C**. **C**, Isolated peak NMDAR oEPSCs from saline-treated animals were significantly more responsive to UBP141 (3  $\mu$ M) compared with cells from carrageenan-treated animals (Student's *t* test unpaired *t* test,  $p = 0.009$ ). **D**, The charge transfer of NMDAR oEPSCs of saline-treated animals was significantly more responsive to UBP141 compared with cells from carrageenan-treated animals (Student's *t* test unpaired *t* test,  $p = 0.0055$ ). **E**, Example oEPSCs before and after bath application of ifenprodil in the same cells from **A**. **F**, Time course of isolated peak NMDAR oEPSCs following bath application of Ifenprodil (10  $\mu$ M), a GluN2B antagonist, quantified in **G**. **G**, There were no significant differences between the peak amplitude oEPSCs from the carrageenan-treated and saline-treated groups in response to ifenprodil (10  $\mu$ M; Student's *t* test unpaired *t* test,  $p = 0.121$ ). **H**, NMDAR oEPSC charge transfer in cells from carrageenan-treated animals was not significantly different in ifenprodil compared with that in cells from saline-treated animals (Student's *t* test unpaired *t* test:  $p = 0.056$ ). \* $p < 0.05$ .

inflammatory pain (Burek et al., 2022). Our work represents a step forward in understanding the complex neurocircuit role of the PAG in affective phenotypes.

### Excitatory drive from PAG to VTA DA neurons

In this study, we also present data supporting the idea that excitatory drive from PAG to dopamine neurons is

unchanged 24 h after carrageenan inflammatory injury. Presynaptic and postsynaptic metrics associated with excitatory neurotransmission did not reveal any differences between cells from carrageenan-treated and saline-treated mice. Although our results do not support the hypothesis of reduced excitatory neurotransmission following acute inflammation, they are concordant with work suggesting that pain and noxious stimuli generally

increases inhibitory neurotransmission onto VTA DA neurons (Markovic et al., 2021; Yang et al., 2021). Our experiments also confirm previous observations showing the presence of GluN2D-containing and Glu2A-lacking glutamate receptors in VTA DA neurons and demonstrating that afferents from the PAG contribute to synapses expressing both receptor subtypes (Jones and Gibb, 2005; Bellone and Lüscher, 2006).

The relevance of circuit-specific complexities cannot be overstated. Of note, in this study we did not patch from the interpeduncular nucleus, rostral linear nucleus, or other rostromedial VTA structures. These structures are thought to contain DA neurons projecting to the medial prefrontal cortex (Beier et al., 2015; Beier et al., 2019), which have increased AMPA/NMDA ratios 24 h following formalin injury (Lammel et al., 2008). Moreover, in our study we have grouped all lateral VTA DA neurons as a single population, despite physiological variation dependent on location within the VTA and projection targets (Lammel et al., 2011; Beier et al., 2015; Morales and Margolis, 2017; Zhang et al., 2017; Huang et al., 2019, 2020). Indeed, in multiple pain models, several groups have shown a reduction in firing rate, AMPA/NMDA ratios, and sEPSCs specifically in the VTA neurons that project to the NAc (Lammel et al., 2011; Ren et al., 2016; Zhang et al., 2017; Markovic et al., 2021). Conversely, VTA neurons projecting to the PFC undergo different alterations such as increased AMPA/NMDA ratios, which is consistent with increased neurotransmission via this pathway following inflammatory pain (Lammel et al., 2008). In light of recently published data concerning other ascending pain pathways to the VTA (Yang et al., 2021), our work highlights that there are parallel streams of ascending pain-relevant information with different magnitudes of injury-induced plasticity.

### Excitatory drive from PAG to VTA GABA neurons

GABAergic neurons in the VTA also may comprise a heterogeneous population, and some of these neurons act locally to inhibit dopamine neurons while others project out of the VTA (Tan et al., 2012; van Zessen et al., 2012; Paul et al., 2018, 2019; Polter et al., 2018; An et al., 2021). Some of our data appear to cluster (Fig. 3F,G, example), possibly suggesting that PAG excitatory synapses on GABAergic subpopulations may exhibit distinct properties. Further work will be needed to clarify the roles of VTA GABA neuron subgroups in inflammatory injury.

Following acute carrageenan inflammation, we identified a decrease in the currents through GluN2D containing NMDARs at these synapses, without observing other significant alterations in metrics of synaptic function. Within the midbrain, GluN2D (but not GluN2C) subunits are expressed postnatally and into adulthood (Monyer et al., 1994; Wenzel et al., 1996). GluN2D receptors generally exhibit reduced  $Mg^{2+}$  block, and do not require depolarization for the influx of calcium, in theory providing a mechanism for tonic NMDAR activity without calcium-dependent inactivation (Gary and Gabriela, 2020). Within midbrain substantia nigra dopamine neurons, NMDARs containing either GluN1/GluN2B or GluN1/GluN2D subunits are expressed postnatally. However, GluN1/GluN2D/

GluN2B triheteromers (i.e., NMDAR heterotetramers containing three different types of GluN subunits) develop in these neurons by P21 (Jones and Gibb, 2005; Brothwell et al., 2008; Suárez et al., 2010; Morris et al., 2018). In undifferentiated midbrain neurons, GluN2D subunits can form these triheteromers with either a GluN2A or GluN2B subunit (Dunah et al., 1998), and these conformations are also found in forebrain inhibitory interneurons (von Engelhardt et al., 2015; Perszyk et al., 2016). Our study is the first to examine these in identified synapses onto VTA GABA neurons.

NMDAR-mediated currents at glutamatergic PAG synapses on VTA GABA neurons from carrageenan-treated animals were less sensitive to the GluN2D-biased antagonist UBP141 ( $3 \mu M$ ) compared with those from saline-treated mice. This was observed despite unchanged AMPA/NMDA ratios and EPSC amplitudes recorded at either  $-70$  or  $+40$  mV. Morris et al. (2018) suggested that in the absence of triheteromeric GluN2D receptors, midbrain dopamine neurons have increased the expression of GluN1/GluN2B NMDA receptors. In contrast, in VTA GABA neurons we saw a trend toward increased sensitivity to the GluN2B-specific antagonist ifenprodil. Because GluN1/GluN2A/GluN2D triheteromers are found in the midbrain, this perhaps suggests that if VTA GABA neurons undergo subunit substitution following acute inflammation they may incorporate GluN2A, rather than GluN2B, subunits.

This change in NMDAR composition coupled with the consistency of baseline neurotransmission, leads to questions about the functional relevance of GluN2D subunits at these synapses. Changes in  $Mg^{2+}$  block and  $Ca^{2+}$  entry will directly affect glutamatergic cellular communication. In the hippocampus, GluN2D subunits contribute to synapse maturation (Yamasaki et al., 2014) and the expression of some forms of plasticity as pharmacological antagonism can reduce the magnitude of short-term potentiation or LTP depending on the stimulation protocol (France et al., 2017; Eapen et al., 2021). However, how these manifest in the midbrain are unknown. Clues may come from work on other  $Ca^{2+}$ -permeable ionotropic glutamate receptors, the GluA2-lacking AMPARs. GluA2-lacking AMPARs and their regulation of  $Ca^{2+}$  influx can serve diverse roles, from an excitotoxic signal (Liu and Zukin, 2007) to induction and maintenance of multiple forms of plasticity (Hage et al., 2016), shaping future signal responses including dendritic spine growth and shrinkage.

Midbrain neurons contain glutamatergic synapses on both the spine and shaft of dendrites (Jang et al., 2015; Hage et al., 2016), with NMDARs recruited preferentially to spine heads. There, in conjunction with voltage-gated sodium channels, they can provide a mechanism for changes in synaptically evoked firing patterns in response to dendritic inputs (Hage et al., 2016). Integrating GluN2D NMDAR into this model is expected to allow  $Ca^{2+}$  entry across a broader range of membrane potentials, thereby promoting higher-frequency firing at rest. Alternatively, GluN2D-containing NMDARs may serve to increase the frequency of  $Ca^{2+}$  transients through these receptors, promoting the maintenance of these synapses; after carrageenan treatment, excitatory synapses from the PAG

may be destined for pruning (Liu and Zukin, 2007). These hypotheses remain untested and present an opportunity for future study.

Together, our results show that following injury, the excitatory PAG synapses on GABAergic neurons of the VTA rather than on DA neurons are selectively modulated through the NMDA receptor. As many of these GABA neurons control DA neuron firing via feedforward inhibition, they could contribute to the reported increase in spontaneous GABAergic IPSCs in DA neurons observed during inflammatory pain (Markovic et al., 2021). Further work will be needed to test whether these initial findings at 24 h following injury are exacerbated in a persistent pain model.

## References

- An S, Li X, Deng L, Zhao P, Ding Z, Han Y, Luo Y, Liu X, Li A, Luo Q, Feng Z, Gong H (2021) A whole-brain connectivity map of VTA and SNc glutamatergic and GABAergic neurons in mice. *Front Neuroanat* 15:818242.
- Basbaum AI, Bautista DM, Scherrer G, Julius D (2009) Cellular and molecular mechanisms of pain. *Cell* 139:267–284.
- Beier KT, Steinberg EE, DeLoach KE, Xie S, Miyamichi K, Schwarz L, Gao XJ, Kremer EJ, Malenka RC, Luo L (2015) Circuit architecture of VTA dopamine neurons revealed by systematic input-output mapping. *Cell* 162:622–634.
- Beier KT, Gao XJ, Xie S, DeLoach KE, Malenka RC, Luo L (2019) Topological organization of ventral tegmental area connectivity revealed by viral-genetic dissection of input-output relations. *Cell Rep* 26:159–167.e6.
- Bellone C, Lüscher C (2006) Cocaine triggered AMPA receptor redistribution is reversed in vivo by mGluR-dependent long-term depression. *Nat Neurosci* 9:636–641.
- Benitz KF, Hall LM (1959) Local morphological response following a single subcutaneous injection of carrageenin in the rat. *Proc Soc Exp Biol Med* 102:442–445.
- Bonin RP, Bories C, De Koninck Y (2014) A simplified up-down method (SUDO) for measuring mechanical nociception in rodents using von Frey filaments. *Mol Pain* 10:26.
- Brischoux F, Chakraborty S, Brierley DI, Ungless MA (2009) Phasic excitation of dopamine neurons in ventral VTA by noxious stimuli. *Proc Natl Acad Sci USA* 106:4894–4899.
- Brothwell SL, Barber JL, Monaghan DT, Jane DE, Gibb AJ, Jones S (2008) NR2B- and NR2D-containing synaptic NMDA receptors in developing rat substantia nigra pars compacta dopaminergic neurons. *J Physiol* 586:739–750.
- Burek DJ, Massaly N, Yoon HJ, Doering M, Morón JA (2022) Behavioral outcomes of complete Freund adjuvant-induced inflammatory pain in the rodent hind paw: a systematic review and meta-analysis. *Pain* 163:809–819.
- Campion KN, Saville KA, Morgan MM (2016) Relative contribution of the dorsal raphe nucleus and ventrolateral periaqueductal gray to morphine antinociception and tolerance in the rat. *Eur J Neurosci* 44:2667–2672.
- de Jong JW, Afjei SA, Pollak Dorocic I, Peck JR, Liu C, Kim CK, Tian L, Deisseroth K, Lammel S (2019) A neural circuit mechanism for encoding aversive stimuli in the mesolimbic dopamine system. *Neuron* 101:133–151.e7.
- Deuis JR, Vetter I (2016) The thermal probe test: a novel behavioral assay to quantify thermal paw withdrawal thresholds in mice. *Temperature (Austin)* 3:199–207.
- Dunah AW, Luo J, Wang YH, Yasuda RP, Wolfe BB (1998) Subunit composition of N-methyl-D-aspartate receptors in the central nervous system that contain the NR2D subunit. *Mol Pharmacol* 53:429–437.
- Eapen AV, Fernández-Fernández D, Georgiou J, Bortolotto ZA, Lightman S, Jane DE, Volianskis A, Collingridge GL (2021) Multiple roles of GluN2D-containing NMDA receptors in short-term potentiation and long-term potentiation in mouse hippocampal slices. *Neuropharmacology* 201:108833.
- France G, Fernández-Fernández D, Burnell ES, Irvine MW, Monaghan DT, Jane DE, Bortolotto ZA, Collingridge GL, Volianskis A (2017) Multiple roles of GluN2B-containing NMDA receptors in synaptic plasticity in juvenile hippocampus. *Neuropharmacology* 112:76–83.
- Gary JI, Gabriela KP (2020) Ca<sup>2+</sup>-Dependent inactivation of GluN2A and GluN2B NMDA receptors occurs by a common kinetic mechanism. *Biophys J* 118:798–812.
- Hage TA, Sun Y, Khaliq ZM (2016) Electrical and Ca(2+) signaling in dendritic spines of substantia nigra dopaminergic neurons. *Elife* 5:e13905.
- Hansen KB, Yi F, Perszyk RE, Furukawa H, Wollmuth LP, Gibb AJ, Traynelis SF (2018) Structure, function, and allosteric modulation of NMDA receptors. *J Gen Physiol* 150:1081–1105.
- Hargreaves K, Dubner R, Brown F, Flores C, Joris J (1988) A new and sensitive method for measuring thermal nociception in cutaneous hyperalgesia. *Pain* 32:77–88.
- Huang S, Borgland SL, Zamponi GW (2019) Peripheral nerve injury-induced alterations in VTA neuron firing properties. *Mol Brain* 12:89.
- Huang S, Zhang Z, Gambeta E, Xu SC, Thomas C, Godfrey N, Chen L, M'Dahoma S, Borgland SL, Zamponi GW (2020) Dopamine inputs from the ventral tegmental area into the medial prefrontal cortex modulate neuropathic pain-associated behaviors in mice. *Cell Rep* 31:107812.
- Hummel M, Lu P, Cummons TA, Whiteside GT (2008) The persistence of a long-term negative affective state following the induction of either acute or chronic pain. *Pain* 140:436–445.
- Jang M, Um KB, Jang J, Kim HJ, Cho H, Chung S, Park MK (2015) Coexistence of glutamatergic spine synapses and shaft synapses in substantia nigra dopamine neurons. *Sci Rep* 5:14773.
- Johnson SW, North RA (1992) Opioids excite dopamine neurons by hyperpolarization of local interneurons. *J Neurosci* 12:483–488.
- Jones S, Gibb AJ (2005) Functional NR2B- and NR2D-containing NMDA receptor channels in rat substantia nigra dopaminergic neurons. *J Physiol* 569:209–221.
- Lammel S, Hetzel A, Häckel O, Jones I, Liss B, Roeper J (2008) Unique properties of mesoprefrontal neurons within a dual mesocorticolimbic dopamine system. *Neuron* 57:760–773.
- Lammel S, Ion DI, Roeper J, Malenka RC (2011) Projection-specific modulation of dopamine neuron synapses by aversive and rewarding stimuli. *Neuron* 70:855–862.
- Lewis VA, Gebhart GF (1977) Evaluation of the periaqueductal central gray (PAG) as a morphine-specific locus of action and examination of morphine-induced and stimulation-produced analgesia at coincident PAG loci. *Brain Res* 124:283–303.
- Li C, Kash TL (2019)  $\kappa$ -Opioid receptor modulation of GABAergic inputs onto ventrolateral periaqueductal gray dopamine neurons. *Mol Neuropsychiatry* 5:190–199.
- Liu SJ, Zukin RS (2007) Ca<sup>2+</sup>-permeable AMPA receptors in synaptic plasticity and neuronal death. *Trends Neurosci* 30:126–134.
- Lowery-Gionta EG, DiBerto J, Mazzone CM, Kash TL (2018) GABA neurons of the ventral periaqueductal gray area modulate behaviors associated with anxiety and conditioned fear. *Brain Struct Funct* 223:3787–3799.
- Madisen L, Zwingman TA, Sunkin SM, Oh SW, Zariwala HA, Gu H, Ng LL, Palmiter RD, Hawrylycz MJ, Jones AR, Lein ES, Zeng H (2010) A robust and high-throughput Cre reporting and characterization system for the whole mouse brain. *Nat Neurosci* 13:133–140.
- Markovic T, Pedersen CE, Massaly N, Vachez YM, Ruyle B, Murphy CA, Abiraman K, Shin JH, Garcia JJ, Yoon HJ, Alvarez VA, Bruchas MR, Creed MC, Morón JA (2021) Pain induces adaptations in ventral tegmental area dopamine neurons to drive anhedonia-like behavior. *Nat Neurosci* 24:1601–1613.
- Mendes-Gomes J, Amaral VCS, Nunes-de-Souza RL (2011) Ventrolateral periaqueductal gray lesion attenuates nociception

- but does not change anxiety-like indices or fear-induced antinociception in mice. *Behav Brain Res* 219:248–253.
- Mirenowicz J, Schultz W (1996) Preferential activation of midbrain dopamine neurons by appetitive rather than aversive stimuli. *Nature* 379:449–451.
- Monyer H, Burnashev N, Laurie DJ, Sakmann B, Seeburg PH (1994) Developmental and regional expression in the rat brain and functional properties of four NMDA receptors. *Neuron* 12:529–540.
- Morales M, Margolis EB (2017) Ventral tegmental area: cellular heterogeneity, connectivity and behaviour. *Nat Rev Neurosci* 18:73–85.
- Morris PG, Mishina M, Jones S (2018) Altered synaptic and extrasynaptic NMDA receptor properties in substantia nigra dopaminergic neurons from mice lacking the GluN2D subunit. *Front Cell Neurosci* 12:354.
- Nair-Roberts RG, Chatelain-Badie SD, Benson E, White-Cooper H, Bolam JP, Ungless MA (2008) Stereological estimates of dopaminergic, GABAergic and glutamatergic neurons in the ventral tegmental area, substantia nigra and retrorubral field in the rat. *Neuroscience* 152:1024–1031.
- Navratilova E, Xie JY, Okun A, Qu C, Eyde N, Ci S, Ossipov MH, King T, Fields HL, Porreca F (2012) Pain relief produces negative reinforcement through activation of mesolimbic reward-valuation circuitry. *Proc Natl Acad Sci USA* 109:20709–20713.
- Ntamati NR, Creed M, Achargui R, Lüscher C (2018) Periaqueductal efferents to dopamine and GABA neurons of the VTA. *PLoS One* 13:e0190297.
- Nugent FS, Niehaus JL, Kauer JA (2009) PKG and PKA signaling in LTP at GABAergic synapses. *Neuropsychopharmacology: Official Publication of the American College of Neuropsychopharmacology* 34:1829–1842.
- Omelchenko N, Sesack SR (2010) Periaqueductal gray afferents synapse onto dopamine and GABA neurons in the rat ventral tegmental area. *J Neurosci Res* 88:981–991.
- Paul EJ, Kalk E, Tossell K, Irvine EE, Franks NP, Wisden W, Withers DJ, Leiper J, Ungless MA (2018) nNOS-expressing neurons in the ventral tegmental area and substantia nigra pars compacta. *eNeuro* 5:ENEURO.0381-18.2018.
- Paul EJ, Tossell K, Ungless MA (2019) Transcriptional profiling aligned with in situ expression image analysis reveals mosaically expressed molecular markers for GABA neuron sub-groups in the ventral tegmental area. *Eur J Neurosci* 50:3732–3749.
- Perszyk RE, DiRaddo JO, Strong KL, Low C-M, Ogden KK, Khatri A, Vargish GA, Pelkey KA, Tricoire L, Liotta DC, Smith Y, McBain CJ, Traynelis SF (2016) GluN2D-containing N-methyl-D-aspartate receptors mediate synaptic transmission in hippocampal interneurons and regulate interneuron activity. *Mol Pharmacol* 90:689–702.
- Polter AM, Barcomb K, Tsuda AC, Kauer JA (2018) Synaptic function and plasticity in identified inhibitory inputs onto VTA dopamine neurons. *Eur J Neurosci* 47:1208–1218.
- Ren W, Centeno MV, Berger S, Wu Y, Na X, Liu X, Kondapalli J, Apkarian AV, Martina M, Surmeier DJ (2016) The indirect pathway of the nucleus accumbens shell amplifies neuropathic pain. *Nat Neurosci* 19:220–222.
- Root DH, Zhang S, Barker DJ, Miranda-Barrientos J, Liu B, Wang H-L, Morales M (2018) Selective brain distribution and distinctive synaptic architecture of dual glutamatergic-GABAergic neurons. *Cell Rep* 23:3465–3479.
- Samineni VK, Grajales-Reyes JG, Copits BA, O'Brien DE, Trigg SL, Gomez AM, Bruchas MR, Gereau RW (2017) Divergent modulation of nociception by glutamatergic and GABAergic neuronal subpopulations in the periaqueductal gray. *eNeuro* 4:ENEURO.0129-16.2017.
- St Laurent R, Martinez Damonte V, Tsuda AC, Kauer JA (2020) Periaqueductal gray and rostromedial tegmental inhibitory afferents to VTA have distinct synaptic plasticity and opiate sensitivity. *Neuron* 106:624–636.e4.
- Stuber GD, Stamatakis AM, Kantak PA (2015) Considerations when using Cre-driver rodent lines for studying ventral tegmental area circuitry. *Neuron* 85:439–445.
- Suárez F, Zhao Q, Monaghan DT, Jane DE, Jones S, Gibb AJ (2010) Functional heterogeneity of NMDA receptors in rat substantia nigra pars compacta and reticulata neurones. *Eur J Neurosci* 32:359–367.
- Suckow SK, Deichsel EL, Ingram SL, Morgan MM, Aicher SA (2013) Columnar distribution of catecholaminergic neurons in the ventrolateral periaqueductal gray and their relationship to efferent pathways. *Synapse* 67:94–108.
- Sun GL, Song ZJ, Peng XH, Chen PP, Song Y, Qin X, Hua R, Zhang YM (2021) Projection-specific dopamine neurons in the ventral tegmental area participated in morphine-induced hyperalgesia and anti-nociceptive tolerance in male mice. *J Psychopharmacol* 35:591–605.
- Tan KR, Yvon C, Turiault M, Mirzabekov JJ, Doehner J, Labouèbe G, Deisseroth K, Tye KM, Lüscher C (2012) GABA neurons of the VTA drive conditioned place aversion. *Neuron* 73:1173–1183.
- Taylor NE, Pei J, Zhang J, Vlasov KY, Davis T, Taylor E, Weng F-J, Van Dort CJ, Solt K, Brown EN (2019a) The role of glutamatergic and dopaminergic neurons in the periaqueductal gray/dorsal raphe: separating analgesia and anxiety. *eNeuro* 6:ENEURO.0018-18.2019.
- Taylor NE, Long H, Pei J, Kukutla P, Phero A, Hadaegh F, Abdelnabi A, Solt K, Brenner GJ (2019b) The rostromedial tegmental nucleus: a key modulator of pain and opioid analgesia. *Pain* 160:2524–2534.
- Ungless MA, Magill PJ, Bolam JP (2004) Uniform inhibition of dopamine neurons in the ventral tegmental area by aversive stimuli. *Science* 303:2040–2042.
- Vaaga CE, Brown ST, Raman IM (2020) Cerebellar modulation of synaptic input to freezing-related neurons in the periaqueductal gray. *eLife* 9:e54302.
- van den Munckhof P, Luk KC, Ste-Marie L, Montgomery J, Blanchet PJ, Sadikot AF, Drouin J (2003) Pitx3 is required for motor activity and for survival of a subset of midbrain dopaminergic neurons. *Development* 130:2535–2542.
- van Zessen R, Phillips JL, Budygin EA, Stuber GD (2012) Activation of VTA GABA neurons disrupts reward consumption. *Neuron* 73:1184–1194.
- von Engelhardt J, Bocklisch C, Tönges L, Herb A, Mishina M, Monyer H (2015) GluN2D-containing NMDA receptors mediate synaptic currents in hippocampal interneurons and pyramidal cells in juvenile mice. *Front Cell Neurosci* 9:95.
- Watanabe M, Narita M, Hamada Y, Yamashita A, Tamura H, Ikegami D, Kondo T, Shinzato T, Shimizu T, Fukuchi Y, Muto A, Okano H, Yamanaka A, Tawfik VL, Kuzumaki N, Navratilova E, Porreca F, Narita M (2018) Activation of ventral tegmental area dopaminergic neurons reverses pathological allodynia resulting from nerve injury or bone cancer. *Mol Pain* 14:1744806918756406.
- Wang MW, Margolis EB, Charbit AR, Fields HL (2019) A midbrain circuit that mediates headache aversiveness in rats. *Cell Rep* 28:2739–2747.e4.
- Wenzel A, Villa M, Mohler H, Benke D (1996) Developmental and regional expression of NMDA receptor subtypes containing the NR2D subunit in rat brain. *J Neurochem* 66:1240–1248.
- Yamasaki M, Okada R, Takasaki C, Toki S, Fukaya M, Natsume R, Sakimura K, Mishina M, Shirakawa T, Watanabe M (2014) Opposing role of NMDA receptor GluN2B and GluN2D in somatosensory development and maturation. *J Neurosci* 34:11534–11548.
- Yang H, de Jong JW, Cerniauskas I, Peck JR, Lim BK, Gong H, Fields HL, Lammel S (2021) Pain modulates dopamine neurons via a spinal-parabrachial-mesencephalic circuit. *Nat Neurosci* 24:1402–1413.
- Zhang H, Qian YL, Li C, Liu D, Wang L, Wang XY, Liu MJ, Liu H, Zhang S, Guo XY, Yang JX, Ding HL, Koo JW, Mouzon E, Deisseroth K, Nestler EJ, Zachariou V, Han MH, Cao JL (2017) Brain-derived neurotrophic factor in the mesolimbic reward circuitry mediates nociception in chronic neuropathic pain. *Biol Psychiatry* 82:608–618.
- Zhao S, Maxwell S, Jimenez-Beristain A, Vives J, Kuehner E, Zhao J, O'Brien C, de Felipe C, Semina E, Li M (2004) Generation of embryonic stem cells and transgenic mice expressing green fluorescence protein in midbrain dopaminergic neurons. *Eur J Neurosci* 19:1133–1140.